Received: 9 September 2016 | Accepted: 24 June 2017

DOI: 10.1111/desc.12602

PAPER

WILEY Developmental Science

Changes in frontal and posterior cortical activity underlie the early emergence of executive function

Aaron T. Buss[1] | John P. Spencer[2]

[1]Department of Psychology, University of Tennessee, Knoxville, TN, USA

[2]School of Psychology, University of East Anglia, Norwich, UK

Correspondence
Aaron T. Buss, 1404 Circle Dr., 301C Austin Peay, University of Tennessee, Department of Psychology, Knoxville, TN 37996, USA.
Email: abuss@utk.edu

Funding Information
This work was supported by National Science Foundation BCS-1029082 awarded to JPS.

Abstract

Executive function (EF) is a key cognitive process that emerges in early childhood and facilitates children's ability to control their own behavior. Individual differences in EF skills early in life are predictive of quality-of-life outcomes 30 years later (Moffitt et al., 2011). What changes in the brain give rise to this critical cognitive ability? Traditionally, frontal cortex growth is thought to underlie changes in cognitive control (Bunge & Zelazo, 2006; Moriguchi & Hiraki, 2009). However, more recent data highlight the importance of long-range cortical interactions between frontal and posterior brain regions. Here, we test the hypothesis that developmental changes in EF skills reflect changes in how posterior and frontal brain regions work together. Results show that children who fail a "hard" version of an EF task and who are thought to have an immature frontal cortex, show robust frontal activity in an "easy" version of the task. We show how this effect can arise via posterior brain regions that provide on-the-job training for the frontal cortex, effectively teaching the frontal cortex adaptive patterns of brain activity on "easy" EF tasks. In this case, frontal cortex activation can be seen as both the cause and the consequence of rule switching. Results also show that older children have differential posterior cortical activation on "easy" and "hard" tasks that reflects continued refinement of brain networks even in skilled children. These data set the stage for new training programs to foster the development of EF skills in at-risk children.

RESEARCH HIGHLIGHTS

- The dimensional change card sort (DCCS) task reveals changes in children's flexible rule-use: 3-year-olds typically fail to switch rules, but 4- and 5-year-olds have little difficulty switching rules.
- Children who fail to switch rules show weak frontal cortex activation; children who switch rules show strong frontal cortex activation.
- We used a dynamic neural field model to explain this brain/behavior relationship and then generated hemodynamic predictions in "easy" and "hard" versions of the DCCS task.
- Using functional near-infrared spectroscopy, we report that children who failed the "hard" version of the task (and showed weak frontal cortex activation when doing so) nonetheless showed strong frontal cortex activation when correctly switching rules in the "easy" version of the task.
- Results also show that older children have differential posterior cortical activation on "easy" and "hard" tasks that reflects continued refinement of brain networks even in skilled children. These data set the stage for new training programs to foster the development of executive function (EF) skills in at-risk children.

1 | INTRODUCTION

Executive function (EF) is a key cognitive process that emerges between 3 and 5 years and facilitates cognitive control and flexible thinking (Carlson, 2005; Zelazo, Muller, Frye, & Marcovitch, 2003).

Previous research has shown a strong relationship between individual differences in EFs during early childhood and later academic achievement as well as quality of life outcomes into adulthood (Eakin et al., 2004; Moffitt et al., 2011), making EF a key target for early intervention efforts (Diamond & Lee, 2011; Heckman, 2011). An initial step to designing effective EF interventions is to understand the developmental mechanisms involved in the emergence of cognitive control. Getting to this point, however, requires a theoretical framework that can specify how neural processes are related to specific cognitive processes. In this paper, we present a neural-based theory of EF—a dynamic neural field (DNF) model—which can simultaneously explain both behavioral and neural mechanisms underlying the development of EF (see Buss & Spencer, 2014). We then test this theory using both behavioral and functional neural measures with 3- and 4-year-old children.

The present study focuses on a canonical task used to assess EF in early development, the Dimensional Change Card Sort (DCCS; see Figure 1a) task (Zelazo, 2006; Zelazo et al., 2003). In this task, children are first instructed to sort cards by one dimension (e.g., color) and then to switch and sort by the other dimension (e.g., shape). Target cards (e.g., a blue circle and a red star) are displayed at sorting locations to show which features go where for the different sets of rules. Children are asked to sort test cards that match either target card along different dimensions, creating conflict when making a decision. For instance, in Figure 1a, one test card (blue star) matches the left target card along the color dimension but matches the right target card along the shape dimension. Performance on this task dramatically changes from 3 to 5 years of age. Typically, the majority of 3-year-olds fail to switch rules, but 4- to 5-year-olds have little difficulty switching to the new rules.

To understand the neural dynamics associated with improvements in the DCCS task, Moriguchi and Hiraki (2009) measured hemodynamic changes using functional near-infrared spectroscopy (fNIRS). fNIRS uses safe, non-invasive near-infrared light to monitor changes in blood oxygenation in the cortical surface (Boas & Franceschini, 2009). Children who successfully switched rules showed robust frontal activation as indexed by large increases in oxygenated hemoglobin, while children who failed this task showed significantly weaker frontal activation. This finding is in line with traditional cognitive theories of EF development which suggest that frontal cortex growth is the critical factor driving the early emergence of EF (Bunge & Zelazo, 2006; Morton & Munakata, 2002).

The developmental story becomes more complicated, however, in light of other behavioral and neural findings. First, young children are able to switch rules in some versions of the DCCS task (Buss & Spencer, 2014; Zelazo et al., 2003). For instance, in a No-Conflict version of the task (see Figure 1b), children sort test cards that match the target cards along both dimensions during a pre-switch phase. During the post-switch phase, the test cards are changed, introducing the same type of conflict present in the Standard task; however, 3-year-olds are now able to switch rules. If it is the case that successful rule switching relies on growth of the frontal cortex, it is not entirely clear how immature 3-year-olds are able to switch rules in these "easy" task variants. The story is more complicated at the neural level.

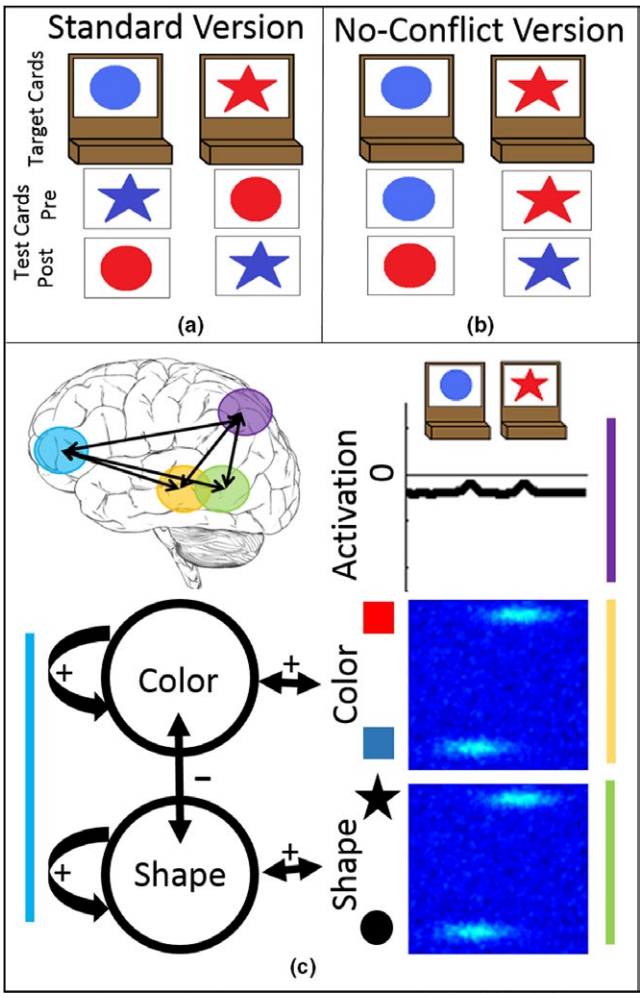

FIGURE 1 Dimensional Change Card Sort Task and Dynamic Neural Field Model. Panel (a) shows the sorting trays, test cards and target cards typically used in the Standard DCCS task. Panel (b) shows the trays, test cards and target cards typically used in the No-Conflict version of the DCCS. Panel (c) shows the DNF model architecture and mapping to cortical regions (see colors on brain inset and vertical colored bars next to the model architecture). The model has task inputs corresponding to the spatial locations and visual features present on the target cards

Research examining the structural and functional development of the brain using MRI suggests that the formation of long-range networks is as important as region-specific measures of growth for cognitive development (Ezekiel, Bosma, & Morton, 2013; Fair et al., 2007, 2008). That is, interactions among frontal and posterior brain regions might be just as important as local changes within frontal cortex in the early emergence of EF. To date, it is unclear what role long-range network interactions play in the early emergence of rule switching. Moreover, because traditional cognitive theories of EF development have emphasized local changes in frontal cortex, they do not provide guidance as to what one might expect from emerging changes in long-range neural interactions.

Novel insights into these questions are offered by a DNF model of the development of EF (Buss & Spencer, 2014). The central idea of

the model is that developmental changes in frontal-posterior neural interactions underlie the emergence of EF between 3 and 5 years. The model hypothesizes that 3-year-olds have weak neural interactions within frontal cortical fields as well as imprecise patterns of connectivity between frontal and posterior cortical fields; 4- to 5-year-olds, by contrast, have stronger frontal neural interactions and more precise frontal-posterior connectivity patterns. When embedded within a real-time neural system, this developmental hypothesis has explained why both young and old children succeed on "easy" versions of the DCCS task, as well as why young children perseverate in most versions of this task. Moreover, the model has generated a series of behavioral predictions that have been successfully tested (Buss & Spencer, 2014; S. Perone, Molitor, Buss, Spencer, & Samuelson, 2015; Sammy Perone, Plebanek, Lorenz, Spencer, & Samuelson, 2017).

Here, we build on this work using a combination of computational and neuroimaging techniques to probe whether coupling between frontal and posterior cortical fields contribute to the emergence of cognitive flexibility in the DCCS task. First, we introduce the DNF model, explaining how changes in frontal-posterior neural activation underlie the development of EF in this model. We then derive hemodynamic predictions from this model in "easy" versus "hard" versions of the DCCS task. Next, we measure the functional brain activity of 3- and 4-year-olds during "easy" and "hard" DCCS tasks using fNIRS. As predicted by the model, we find that early in development in "easy" EF tasks, posterior cortices drive frontal activation in a bottom-up manner. As EF skills are refined over development, this pattern switches to a more adult-like pattern where frontal cortex exerts a top-down influence on posterior cortices, facilitating rule switching in both "easy" and "hard" tasks.

2 | THE DYNAMIC NEURAL FIELD MODEL

DNF models are composed of neural fields that are tuned to continuous dimensions such as color or space. Lateral interactions within each cortical field are governed by a local-excitation/lateral-inhibition function that creates localized "peaks" of activation that reflect, for instance, decisions about the color or shape of a stimulus. Peaks also drive the accumulation of memory traces that increase the baseline activation within cortical fields, facilitating the subsequent activation of neural units over learning. For example, the formation of an activation peak encoding the features of a red stimulus will lead to the accumulation of memory traces for the red feature value that will lead to more rapid peak formation for red stimuli in future instances.

Neural fields can be combined together to build neural architectures that are capable of performing cognitive tasks. Figure 1c shows the DNF model proposed by Buss and Spencer (2014) to explain the development of rule-use in the DCCS task. The model is composed of neural fields corresponding to frontal, parietal, and temporal regions as illustrated by the color coding on the brain image (see Supplemental Materials full model specifications). The parietal and temporal components engage in object representation processes that bind shape and color features to spatial locations when making decisions in the task. These components are reciprocally connected along the spatial dimension (see x-axis in the cortical fields on the right side of Figure 1c). The parietal component (purple; top right panel in Figure 1c) is composed of a population of neural units that are tuned to the spatial dimension. This field forms representations of the spatial locations where the test cards are sorted (i.e., the sorting tray locations). The temporal component is composed of two populations of neural units that separately encode color-space (yellow) conjunctions or shape-space (green) conjunctions. That is, these populations bind shape and color features (see y-axes) to the spatial dimension (x-axes) of the task.

The frontal component implements a form of dimensional attention through connections to posterior cortical fields. Specifically, this component is composed of units that capture the labels "shape" and "color". These units receive task-specific input based on instructions to sort by shape or sort by color and have self-excitatory connections and mutual inhibitory connections that create "peaks" of activation. These units are reciprocally coupled to the temporal components that encode the associated feature dimension. In particular, the "shape" unit is connected to the shape field in the temporal component and the "color" unit is connected to the color field in the temporal component. When instructed to sort by color, the "color" unit becomes activated in the frontal component which boosts the processing of colors in the temporal component and facilitates color-based sorting decisions.

Neural interactions between the frontal and temporal components are reciprocal in nature (see bi-directional arrow in Figure 1c). This allows emerging sorting decisions in the temporal cortical fields to have a "bottom-up" influence, increasing activation in the frontal system and recruiting attentional resources. Without these temporal-to-frontal connections, the model fails to activate the frontal system and is unable to build response peaks. In addition, the "color" and "shape" units also impact processing in parietal cortex. Both units homogenously boost activity of the parietal field to facilitate the formation of a spatial response peak. Finally, the frontal component also accumulates memory traces as the "shape" and "color" units are activated over the course of a simulation.

Figure 2 illustrates the moment-to-moment dynamics that unfold as the model performs the DCCS task. The top panel shows the activation of the dimensional attention units in a "young" model over the course of six pre-switch and six post-switch trials. Figure 2a–j in the middle panel shows snap-shots of the parietal and temporal components of the model at particular moments in this time-course. The bottom panel shows the activation of the dimensional attention units in an "old" model over the course of six pre-switch and six post-switch trials. To highlight how the model works, we step through Figure 2 as key events unfold across the pre- and post-switch trials.

Figure 2a shows the model at the start of a simulation with only the task inputs presented. The spatial field has inputs at a left and right location (note the bumps in activation) corresponding to the locations of the sorting trays. The color field has inputs at the left and right locations for the blue and red target card features, respectively. Likewise, the shape field has inputs at the left and right locations for the circle and star target card features, respectively. These task inputs "pre-shape" the activation of the parietal and temporal

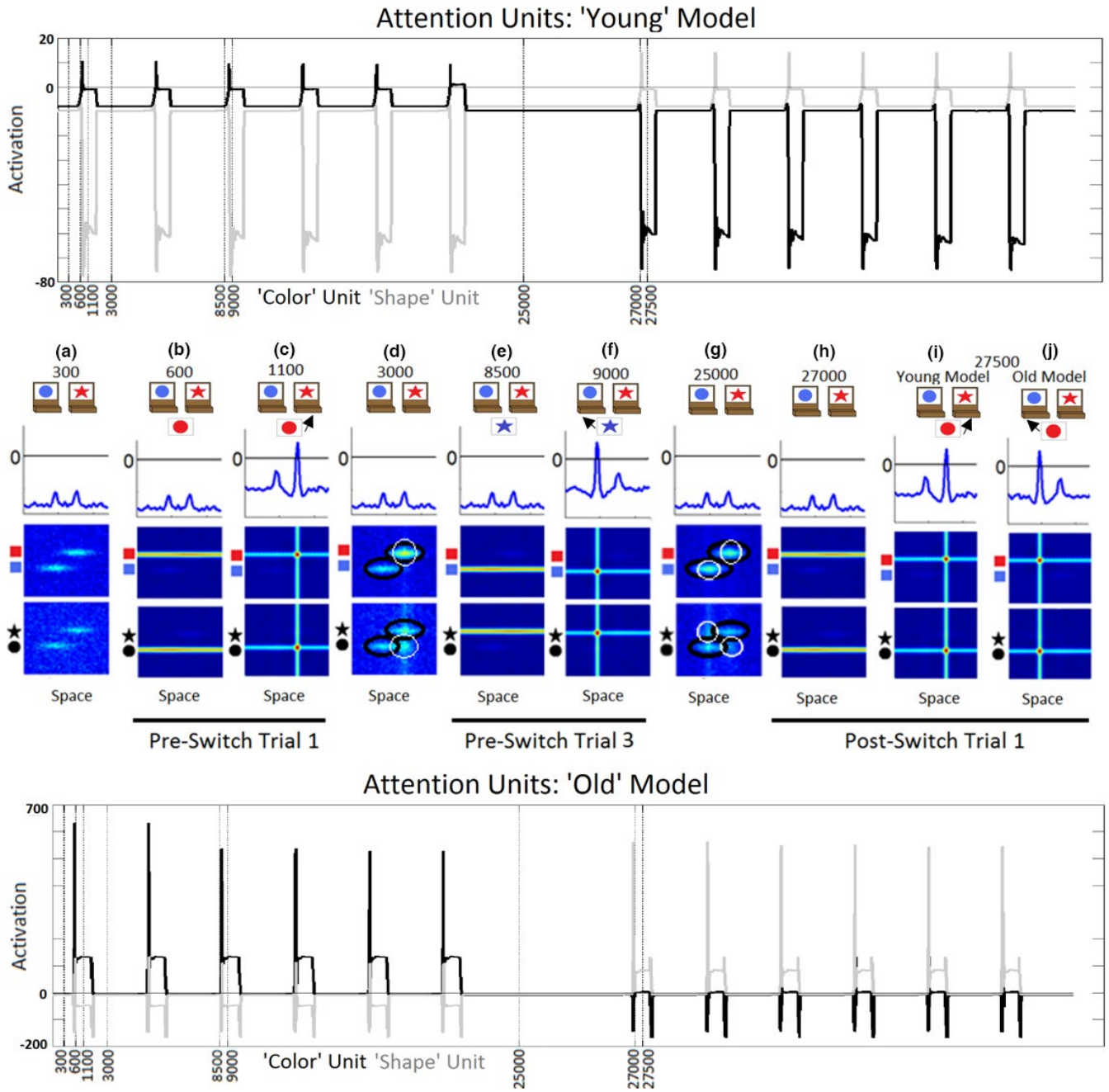

FIGURE 2 Model performing the DCCS task. The top and bottom panels show the activation of the attention units in the frontal component over the course of the pre- and post-switch phases. Panels a–j show images of the parietal and temporal components at different time points. Panel (a) shows the model with the inputs for the target cards and sorting trays. Panel (b) shows the model just after the first test card has been presented to the model. Panel (c) shows the model making a sorting decision on the first trial. Panel (d) shows the model with the memory traces accumulated during the first trial. Panel (e) shows the model just after the third pre-switch test card has been presented. Panel (f) shows the model making a sorting decision during the third pre-switch trial. Panel (g) highlights the configuration of test inputs and memory traces just before the start of the post-switch phase. Panel (h) shows the model just after the first post-switch test card has been presented. Panel (i) shows the "young" model perseverating during the first post-switch trial. Panel (j) shows the "old" model correctly switching rules during the first post-switch trial

object representation system based on structure available in the task space.

The model makes decisions in this task by building peaks of activation across the parietal and temporal components that are tuned to the features on the test card and the location of the response. Figure 2b shows the model just after a red-circle test card has been presented. These test card inputs activate the color and shape features across all spatial locations (see horizontal "ridge" of input at the red value and the circle value)—the test card does not contain any spatial information regarding where it is to be sorted. The decision

about where to sort the card emerges through the spatial coupling among the parietal and temporal cortical fields. Figure 2c shows the sorting behavior on this trial which occurs at time-step 1100. At this point in time, the attention unit for "color" (black line) in the top plot is near the activation threshold whereas the attentional unit for "shape" (gray line) is further below the activation threshold. This boosts the color-space field slightly and activation at rightward location wins the competition because of the presence of a red target card at the right location. This yields a pattern of peaks at the rightward location in the parietal and temporal components (see red dot within the shape and color fields).

Figure 2d highlights the memory traces that form as a result of this decision. In this panel, the target inputs are outlined in a black oval and the memory traces are outlined in a white circle. In the color-space field, there is cooperation: neurons tuned to the red feature at the rightward sorting location are boosted because the memory trace overlaps with the target input. In the shape-space field, however, there is competition: neurons tuned to the circle feature at the rightward location are boosted because of the memory trace but neurons tuned to the circle feature at the leftward location are boosted by the target input. Figure 2e–f shows a similar pattern of events unfolding as the model sorts the blue-star test card during the third pre-switch trial. By the end of the six pre-switch trials, displayed in Figure 2g, the model will have a pattern of cooperation within the color-space field and a pattern of competition within the shape-space field.

In Figure 2h, the model is shown a red-circle to sort on the first post-switch trial. The model has been told to play the "shape" game and the "shape" unit has been activated (see gray line in the top panel). Even though the "shape" unit is more active, Figure 2i shows a perseverative response—the model sorts the red-circle to the right. This reflects the cooperation in the color-space field that boosts sorting red things to the right relative to the competition in the shape-space field which fails to specify where the circle should be sorted. In this situation, decisions are made based on the parietal and temporal fields even though the correct dimensional unit is being activated (see top panel).

To implement development and create an "old" model, parameters are changed to increase the strength of neural interactions within the frontal component and increase the strength and precision of connectivity between the frontal and posterior components of the model. Specifically, we made an "old" model that has stronger local-excitation/lateral-inhibition between the "shape" and "color" nodes. In addition, this model was also given stronger reciprocal connectivity between the "color" node and color-space and spatial fields and between the "shape" node and shape-space and spatial fields.

The bottom panel in Figure 2 shows the activation of the dimensional units for the "old" model. With stronger self-excitation and mutual inhibition, the dimensional units undergo larger changes of activation in the "old" model. This creates more rapid and selective activation of the relevant dimensional unit. In addition, this "old" model has stronger reciprocal coupling with the feature-space fields in the temporal component. As a result of this coupling, the shape-space field is boosted more strongly and more quickly during the post-switch phase. Figure 2j shows the "old" model on a trial during the post-switch phase. Here, the model is able to overcome the competition in the shape-space field and makes a correct decision to sort the red-circle test card to the left.

Buss and Spencer (2014) demonstrated that simulations of the "young" and "old" models explained the performance of 3- to 5-year-olds across 14 different versions of the DCCS based on these principles of local-tuning in frontal cortex, frontal-posterior coupling, and the configuration of memory traces relative to the structure of the task. Importantly, performance of the young model can be facilitated if memory traces are supportive of the task structure during the post-switch phase. In one example, the model explains both why young children fail in the Standard version of the DCCS task (Figure 1a), and why they succeed in a No-Conflict version (Figure 1b: sorting no-conflict cards during the pre-switch phase creates memory traces that support correct sorting during the post-switch phase; see Buss & Spencer, 2014). Repeatedly sorting the *blue-circle* to the left using color rules during the pre-switch phase would support sorting *red-circle* to left when using shape rules in the post-switch phase, because in both cases, circles go to the left (see Figure 1b). The "young" DNF model is able to switch rules in the No-Conflict version at a rate similar to 3-year-olds. This constitutes an important theoretical advance. For instance, although the connectionist model of Morton and Munakata (2002) quantitatively captures rates of switching between 3- and 5-year-olds in the Standard version, this model does not explain the success of 3-year-olds in the No-Conflict version.

3 | USING THE DNF MODEL TO SIMULATE HEMODYNAMIC RESPONSES

We use a model-based approach to neuroimaging (Buss, Wifall, Hazeltine, & Spencer, 2014; Wijeakumar, Ambrose, Spencer, & Curtu, 2017) to simultaneously generate behavioral and hemodynamic data from the DNF model to explain and predict brain–behavior relationships as EF develops. Typically, in task-based functional neuroimaging, researchers examine how neural activity varies across conditions. Because they do not have a quantitative assessment of the neural activity predicted from a theory or model, a common approach is to use a place holder that reflects the timing of stimulation (Anderson, Qin, Jung, & Carter, 2007) or a proxy of some expected hemodynamic activity (Herd, Banich, & O'Reilly, 2006). The data are then analyzed using this basic information and neural processes are inferred in a data-driven, post-hoc manner.

Here, we take an alternative approach, generating neural activity in real time from the model and constructing a priori hemodynamic predictions that can then be directly compared to actual brain measures. In particular, we record simulated neural activity from the model across different conditions and then convolve this neural activity with a blood flow response. We then test whether the brain's blood flow response varies across conditions in the manner predicted by neural activity generated from the model.

As a first step toward this goal, we examined the hemodynamic responses in the Standard DCCS task from the "young" model that

fails to switch rules and the "old" model that correctly switches rules. The goal was to assess whether the model shows neural patterns similar to results reported by Moriguchi and Hiraki (2009). In particular, does the "young" model that perseverates in the Standard DCCS task show weaker hemodynamic signals from the frontal component of the model compared to the "old" model that switches rules in this version of the task? In a second step, we generated predictions regarding the pattern of hemodynamics associated with frontal, parietal, and temporal cortical fields in the Standard and No-Conflict version of the DCCS. We then tested these predictions in an fNIRS study with 3- and 4-year-olds.

4 | SIMULATION METHODS

Simulations were conducted in Matlab 7.5.0 (Mathworks, Inc.) on a PC with an Intel® i7™ 3.33 GHz quad-core processor. The "young" and "old" models were given the Standard and No-Conflict versions of the DCCS task. The full set of parameters for the model is shown in Tables S1–S3. The equations were the same as reported by Buss and Spencer (2014).

As in Buss and Spencer (2014), the model was given six trials during each of the pre- and post-switch phases. Throughout each simulation, target inputs were presented at specific feature and spatial values to capture the relevant details of the target cards for the pre-switch and post-switch phases. At the start of each trial, the model was presented with ridges of input for the features displayed on the test cards. Each trial was simulated for 1500 time-steps, with the test card stimulus presented for 1000 time-steps. The models always generated an active response by the end of this 1000 time-step interval. For the purpose of mapping the real-time simulated neural dynamics to fNIRS data, 1 time-step is equivalent to 2 ms. The old and young models were iterated for 20 runs (corresponding to 20 participants) for each condition (Standard and No-Conflict). Data reported below were averaged over the 20 runs (i.e., 20 individuals). Typically, variations in parameters are used to reflect variations across children. However, the DNF model is stochastic and generates variations in performance across repeated iterations that, in previous work, has mimicked differences in performance across children. Thus, the model was iterated with the same parameters across runs.

To simulate real-time hemodynamics using the DNF model, we adapted an approach from the literature. Logothetis, Pauls, Augath, Trinath, and Oeltermann (2001) recorded single- and multi-unit data along with local field potentials (LFP) and the BOLD signal in visual cortex of macaques. An LFP is a measure of dendritic activity over a localized population of neurons, accounting for changes in both inhibitory and excitatory ion flow. The LFP provides a measure of the input to, and local processing within, a region of cortex. Logothetis et al. (2001) reported that the LFP was most strongly correlated with the BOLD response compared to single- and multi-unit activity. The authors were able to reconstruct the BOLD signal by convolving the LFP with an impulse response function (specifying blood flow response to neural activity), suggesting that the LFP is a strong contributor to the neural signal driving the BOLD response.

DNF models simulate cognitive and behavioral processes using neural population dynamics, uniquely situating such models as bridges between behavioral and neural data (Buss, Wifall et al., 2014; Wijeakumar et al., 2017). Following the approach above, we created a DNF-LFP measure by summing the absolute value of all terms contributing to the rate of change in activation within each component of the model, excluding the stability term and the two factors that impact the neuronal resting level—a resting-level parameter and the memory traces. The included terms reflect excitatory and inhibitory interactions within each component of the model, the excitation that passes between components of the model, and noise. This measure of real-time neural activity was then convolved with a general impulse response function. The hemodynamic response calculated from each component of the model was normalized by dividing by the maximum signal from that component across runs of the model. The average response on each trial was then calculated as a change relative to the pre-trial baseline by setting each trial to begin at a value of 0. The hemodynamic responses for each condition of the "young" and "old" models were then calculated as the average across trials.

5 | RESULTS

Both the "young" and "old" models sorted correctly on all trials during the pre-switch phases of the Standard and No-Conflict conditions. The "old" model sorted correctly on all trials during the post-switch phase of both tasks. The "young" model, however, sorted correctly during all trials of the No-Conflict condition but sorted incorrectly on all trials during the post-switch phase of the Standard task. Thus, the model produced a pattern of behavior that is similar to the behavior of 3- and 4-year-olds, allowing us to examine the neural responses underlying the key trials of interest.

Figure 3 shows multiple novel model-based hemodynamic predictions from the Standard and No-Conflict conditions using the "young" and "old" models. First, we note that the model replicates the pattern reported by Moriguchi and Hiraki (2009) in the Standard condition: The "young" model shows weaker frontal activation when perseverating on post-switch trials compared to the "old" model when switching on post-switch trials. The latter effect reflects the combination of stronger recurrent interactions in frontal cortex and stronger frontal-posterior connectivity for the "old" model. Critically, these findings in the No-Conflict condition set the stage for a novel prediction—*the "young" model shows a robust frontal response when correctly switching in the No-Conflict condition even with an "immature" frontal cortex*. In this No-Conflict condition, memory traces in the posterior cortical fields support correct responding, resulting in a *stronger bottom-up signal being sent from temporal to frontal cortical fields* in the No-Conflict condition relative to the Standard condition.

Figure 4 illustrates this influence by plotting the average strength of activation projected from the post-switch feature field to its dimensional unit (red lines) and from the dimensional units to the feature

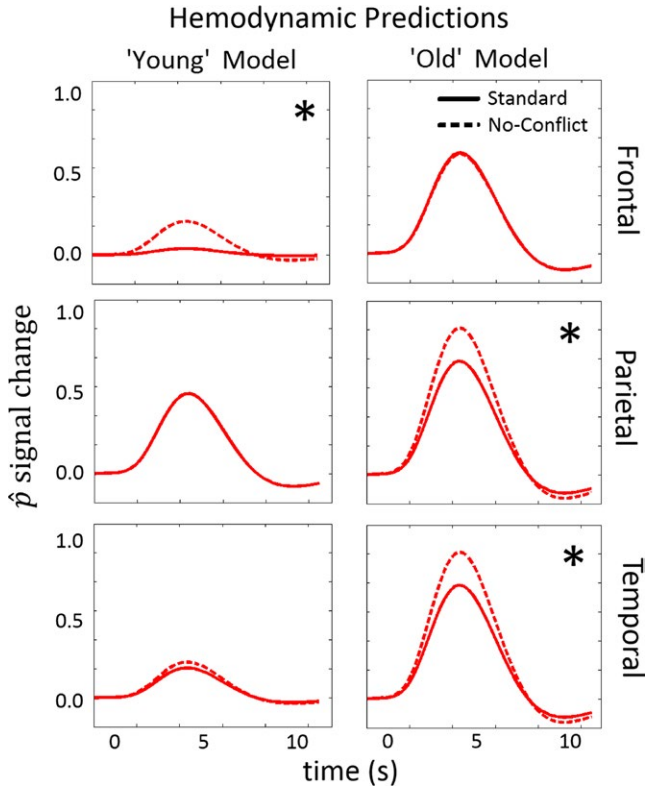

FIGURE 3 Hemodynamic predictions from the DNF models. The model makes a pattern of hemodynamic predictions from the frontal (top), parietal (middle) and temporal (bottom) components of the DNF model. Asterisks mark components that show a significant difference in activation between conditions

fields (blue lines). In the "young" model plotted on the left, the activation from the temporal component is engaged sooner than the feedback activation from the frontal component to the feature field (see activation highlighted in the box on the left). Moreover, the input from the feature fields builds more quickly in the No-Conflict condition (dashed lines) relative to the Standard condition (solid lines). This difference leads to more robust engagement of the frontal units in the No-Conflict condition.

The second novel prediction is that posterior cortical activation will be larger for children who switch rules compared to children who perseverate. As can be seen in Figure 3, the "old" model also shows stronger activation in parietal and temporal cortical fields compared to the "young" model. Thus, developmental changes in neural activation in the DCCS task are not isolated to the frontal cortex. Specifically, stronger coupling between frontal and posterior cortical fields over development results in a *stronger top-down signal from frontal to posterior cortical fields on post-switch trials*. This finding is consistent with data showing robust posterior cortical activation during rule switching in the DCCS with adults (Morton, Bosma, & Ansari, 2009). Figure 4 illustrates this influence by plotting the average strength of activation projected from the dimensional units to their feature fields and vice versa. In contrast to the "young" model, the "old" model engages activation from the dimensional units to the feature fields sooner than it engages activation from the feature fields to the dimensional units. Thus, the frontal component in the "old" model provides an initial "top-down" influence on emerging posterior cortical activation.

The final novel prediction of the model is that children who switch rules in the Standard DCCS condition will show stronger activation in posterior cortical areas in the No-Conflict condition (see Figure 3). Even though older children are able to switch rules, the model predicts that there are critical developmental changes still emerging in the brain. This prediction results from greater stability in the activation of the frontal system in the No-Conflict condition. Figure 4 illustrates this influence by plotting the time-course of activation passed between the feature fields and dimensional units. The input from the dimensional units to the feature fields is stronger in the No-Conflict condition relative to the Standard condition. In the "old" model, this difference drives a boost in the parietal and temporal hemodynamics in the No-Conflict condition. Note that there is also a greater frontal-to-temporal input in the No-Conflict condition in the "young" model; however, this input is much weaker (note the difference in scale) and, consequently, has little impact on posterior hemodynamic activity.

Considered together, predictions 1 and 3 generate a developmental crossover in the locus of condition-specific effects. The model predicts a difference in neural activation between conditions in frontal cortex in early development and a difference in neural activation between conditions in posterior cortices later in development.

6 | TESTING PREDICTIONS OF THE DNF MODEL WITH FNIRS

We tested these predictions with young children using functional near-infrared spectroscopy (fNIRS) with sensors over frontal, temporal, and parietal cortex. Children completed an innovative version of the DCCS task with a continuous, event-related design. Importantly, this design yielded neural data from multiple switch trials across different conditions. Thus, this task provides the first paradigm that allows for comparison of behavioral and neural measures across multiple switch types within the same group of children. Note that the continuous event-related design necessitates the inclusion of blocks of trials that are not of interest to the current study, but instead provide the pre-switch condition for the target post-switch trial blocks.

In the analyses below, we examine whether our data replicate the findings of Moriguchi and Hiraki (2009): do children who perseverate in the Standard task show weaker frontal activation compared to children who switch rules in the Standard task? Next, we examined whether children's hemodynamic responses reflected the three predictions of the DNF model described above. First, for children who perseverate in the Standard task, do we observe stronger frontal activation when correctly switching rules in the No-Conflict version compared to when perseverating in the Standard version? Second, for children who switch rules in the Standard task, do we observe activation in temporal and parietal regions? Third, for children who switch in the Standard task, do we observe stronger activation in the No-Conflict version compared to the Standard version in parietal and temporal regions?

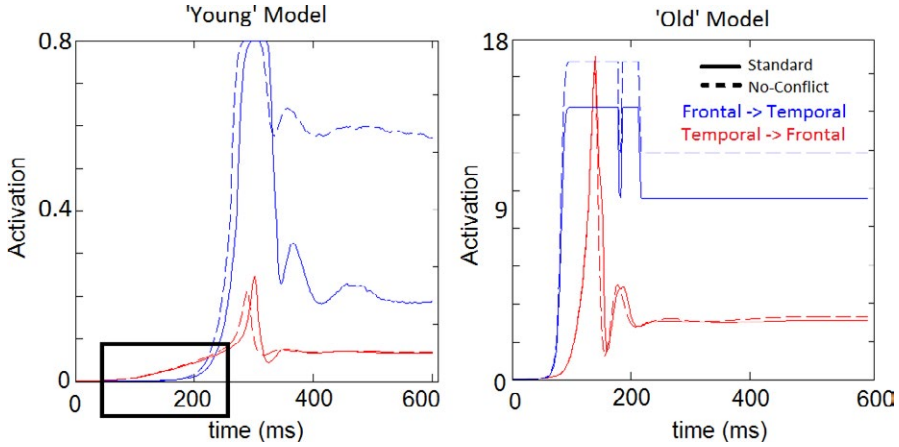

FIGURE 4 Frontal-temporal interactions. Activation strengths between the frontal and temporal components are plotted for the "young" and "old" model in post-switch trials during the Standard and No-Conflict conditions. For the "young" model, activation along the temporal-to-frontal connection begins before the activation along the frontal-to-temporal connection. Additionally, activation in the No-Conflict condition peaks before activation in the Standard condition. For the "old" model, activation along the frontal-to-temporal connection begins before activation along the temporal-to-frontal connection. In addition, activation along the frontal-to-temporal connection is stronger in the No-Conflict condition than in the Standard condition

6.1 | Participants

A sample of 40 children between 40- and 56-months (*M* age = 48.3 months, *SD* age = 6.1 months; 19 males, 21 females) participated. They were recruited from the Iowa City community. Parents were compensated with $10 per hour in the lab and children were given a toy valued at $5 for each visit. Children completed two 1.5 hour sessions which were separated by no more than one week. To be able to identify the neural correlates of behavior in our task, we grouped participants based on their performance. Children who sorted fewer than 50% correct in the Standard condition were categorized as *Perseverators* (*M* age = 44.4 months) and children who sorted better than 50% correct in the Standard condition were categorized as *Switchers* (*M* age = 50.4 months).

6.2 | Behavioral task

Before starting the experiment, children were familiarized with the DCCS task with physical cards and trays. Children were first shown the trays and target cards and were told that they were going to play a set of matching games. In this familiarization phase, children were instructed for either the shape or color game (whichever dimension they would start with in the computerized task). For instance, children who had the color task in the initial phase of the computerized task were told, "You're going to play a matching game. This is called the color game. In the color game, you are going to match by color. All of the blue ones go here and all of the red ones go there." The child was then shown a demonstration of how to sort each test card. The experimenter then gave the child five cards to sort, one at a time, prompting the child by saying "Where does this one go in the color/shape game?" For all trials, the experimenter repeated the rules if the child sorted incorrectly.

After the familiarization trials, the experimenter initiated the computerized version. Children completed the experimental task on a 46″ LCD television monitor that was connected to a computer running E-Prime 2.0 software (Psychology Software Tools, Pittsburgh, PA). Stimuli consisted of 13 different sets of colored shapes.

The behavioral task was constructed to allow for comparison of performance and hemodynamic responses during the Standard and No-Conflict conditions. To achieve this, the pre-switch and a post-switch phase of these conditions were administered in a continuous design that would create multiple iterations of both conditions as illustrated in Figure 5. Each phase contained three trials. We used the same Standard and No-Conflict conditions as used in previous experiments (Buss & Spencer, 2014; Zelazo et al., 2003). Specifically, in the Standard condition, the test dimension changed between the pre- and post-switch phases (sort by color or shape) and the test cards matched either target card in both the pre- and post-switch phases (e.g., a red book and blue circle served as the target cards and a blue book and red circle served as the test cards). In the No-Conflict condition, the test dimension changed, test cards during the pre-switch phase only matched one target card, and the test cards during the post-switch phase were changed to match either target card along different dimensions (e.g., a pink bug and an orange guitar served as both the target and test cards during the pre-switch phase, and the test cards were changed to a pink guitar and an orange bug during the post-switch phase).

Our design differed from previous studies such that these conditions were administered sequentially over many iterations in order to produce many switch trials which could be included in the neural analyses. Thus, each child was given both conditions repeatedly in alteration. To enable this, we conducted sequences of phases where each phase of three trials both served as the pre-switch phase for the next condition and as a post-switch phase relative to the just-previous block of trials. Figure 5 shows an exemplary sequence. In Figure 5a, the child sorts by color with standard cards that have conflict along both shape and color dimensions. In Figure 5b, the rule is changed and

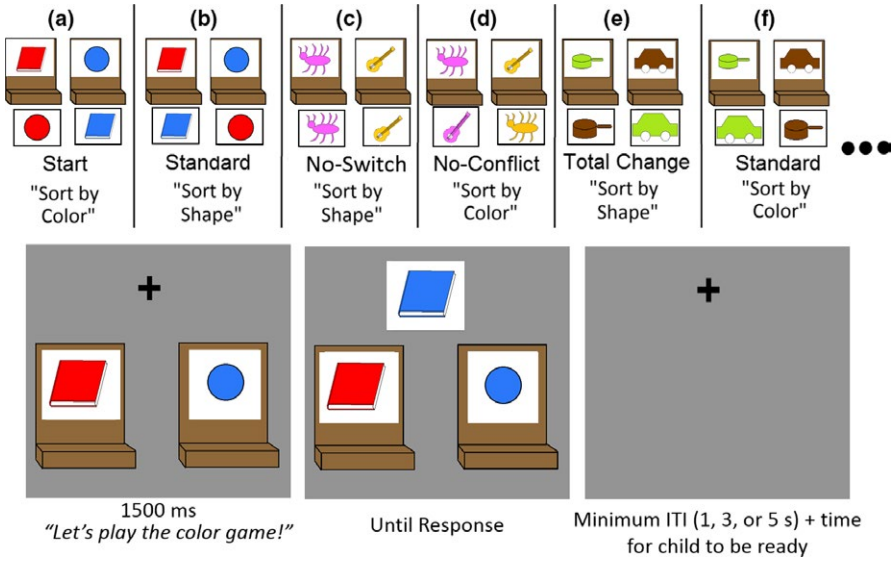

FIGURE 5 Behavioral task. Top panel shows example sequence of sorting phases. Each phase contained three trials. Panel (b) shows the switch phase for the Standard condition. Here, the relevant dimension has changed from the previous phase in Panel (a) and the features have all remained the same so that the test cards need to be sorted to different locations between (a) and (b). Panel (d) shows the No-Conflict switch condition. As with the Standard condition, the relevant dimension has changed. The just previous phase in Panel (c) contained no conflict cards. Thus, the transition from Panel (c) to Panel (d) characterizes the No-Conflict condition as illustrated in Figure 1b. Panel (c) shows the No-Switch condition (which serves as the pre-switch phase for the No-Conflict condition. The bottom panel shows the sequence of events on each trial

the child is asked to sort the cards by shape. Thus, the trials across panels A and B implement the Standard DCCS condition. In Figure 5c, the target cards are changed completely, they match along both dimensions so there is no dimensional conflict, and the child sorts by shape. This phase serves as the pre-switch to the No-Conflict condition. The post-switch phase is shown in Figure 5d. Here, children sort by color, and conflict is introduced between the target cards and the test cards. In Figure 5e, the target and test cards are completely new and children are asked to sort by shape. This replicates a Total Change condition previously administered by Zelazo et al. (2003). Finally, in Figure 5f, the rule is changed—children are asked to sort by color—which constitutes the second phase of the Standard DCCS task.

Note that the design was constructed so that the relevant dimension for each condition alternated between shape and color each time it was presented. For example, in Figure 5, the first Standard phase (Figure 5b) uses shape as the test dimension, while the second Standard phase (Figure 5f) uses color as the test dimension. Similarly, the No-Conflict phase in Figure 5d uses color as the test dimension and the subsequent No-Conflict phase would use shape as the relevant dimension.

During each visit, participants completed two runs through the full design. During each run, they completed each of the four conditions (Standard, No-Switch, No-Conflict, and Total Change) three times in addition to one Start phase that initialized each run and served as the pre-switch phase of the first Standard condition phase, resulting in a total of 13 phases. As mentioned above, each phase contained three trials. Thus, across the two visits, participants completed a total of 156 trials (3 trials per phase × 13 phases × 2 runs × 2 visits).

Trial onsets were synchronized with the fNIRS data collection computer. Each trial began with the presentation of the target cards and sorting trays. At this time, on the first trial of each phase, the experimenter told the child the rules for the game (e.g., "We're going to play the color game. In the color game we sort by color. All of the red ones go here, but all of the blue ones go there."). The rules were also repeated after a card was sorted incorrectly. The experimenter then pressed a button to initiate the trial with an auditory dimensional cue saying, "Let's play the color/shape game!" (see bottom panels of Figure 5). This dimensional cue lasted 1500 ms after which a test card appeared above the center of the screen. The test card remained on the screen until the child responded by pointing to the location where it should be sorted. The experimenter then recorded this response by pushing a left or right response key. After the response was recorded, the screen was blanked for an inter-trial interval (ITI) of either 1, 3, or 5 seconds. Once the child was oriented toward the screen and prepared for the next trial, the experimenter initiated the next trial by pressing a button to display the next set of target cards on the monitor.

6.3 | fNIRS method

NIRS data were collected at 25 Hz using a 36-channel TechEn CW6 system with wavelengths of 830 nm and 690 nm. Light was delivered via fiber optic cables that terminated in a customized cap (Figure 6c) placed on the head with sources and detectors secured within six flexible plastic arrays. The NIRS data were split into 12 regions composed of the 3-channel sets depicted in Figure 6b and different participants were allowed to contribute data for each region (Buss, Fox, Boas, & Spencer, 2014). We refer to these 3-channel sets using the 10–20 sites they were placed over and the channel number. For instance, the 3-channel array near F5 is referred to as F5-1, F5-2, and F5-3 (see Figure 6b). fNIRS measures changes

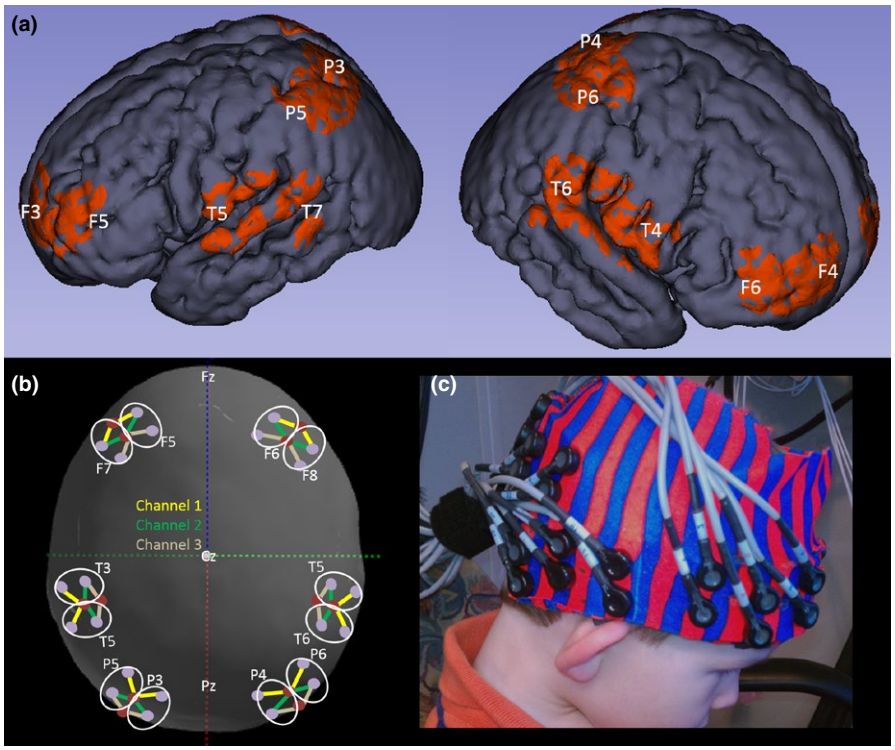

FIGURE 6 fNIRS probe. (a) shows a digital projection of the fNIRS probe onto a standard brain atlas. (b) Shows the numbering scheme for the channels at each region (see Table 1). (c) Shows a photo of a participant wearing the fNIRS probe

in oxygenated hemoglobin (HbO) and deoxygenated hemoglobin (HbR) separately. If a region is activated, then the HbO and HbR signals would be significantly different from each other with HbO at higher levels of concentration than HbR (Buss, Fox et al., 2014). Thus, in the analyses below, we determine which channels are activated across the different conditions of the task by examining whether HbO is greater than HbR.

An initial behavioral criterion was set to include trials in the NIRS analyses. Specifically, each phase of three trials was categorized as "correct" if at least 2/3 were sorted correctly; phases were categorized as "incorrect" if at least 2/3 were sorted incorrectly. Only NIRS data from incorrect trials were included from "incorrect" phases, and only NIRS data from correct trials were included from "correct" phases. This was to yield a cleaner estimate of the hemodynamic profile associated with different trial types. Importantly, we only included data from "valid-switch" phases, that is, only if children sorted 2/3 of the cards correctly on the previous phase. This was done to ensure that we measured neural dynamics associated with the need to switch attention between dimensions.

Using HomER2 software (Huppert, Diamond, Franceschini, & Boas, 2009), the mean baseline was subtracted and data were converted into an optical density measure. Data were then band-pass filtered to remove frequencies slower than .016 Hz and faster than 2 Hz. Two Hz was used as the low pass filter in this initial step to preserve high frequency fluctuations that could be due to motion. In the next step, motion artifacts were removed from each region by eliminating trials with a change in optical density larger than 0.3 absorbance units within the time-window between 2 seconds before to 12 seconds after the onset of the dimensional cue. Data were then band-pass filtered again to retain only frequencies between .016 and .5 Hz. Concentration data were computed using the modified Beer-Lambert Law and the known extinction coefficients of oxygenated and deoxygenated hemoglobin (Boas et al., 2001). Finally, outlier trials were removed on a region-by-region basis. Outliers were identified as trials that contained amplitudes of oxy-Hb that were more than 2.5 standard deviations above or below a participant's mean in each condition for nine consecutive time-samples (a duration of 360 ms). Table 1 shows the number of included participants and average trial counts included in the fNIRS analyses for each condition and each channel.

The average of the hemodynamic response (HbO, HbR) was weighted by the number of trials (Buss, Fox et al., 2014) to reduce the possibility that statistically significant effects are driven primarily by participants with few trials. For statistical analyses, the mean weighted average was computed within an 8 second time-window spanning 2 seconds after the dimensional cue to 10 seconds after dimensional cue. The average time between trials was 13.7 seconds (*SD* = 3.9 s) for *Perseverators* and 10.3 seconds (*SD* = 2.6 s) for *Switchers*. Importantly this time-window captures the peak response on each trial, which typically occurs 7–8 seconds post stimulus onset (Schroeter, Zysset, Wahl, & von Cramon, 2004). Hemodynamic responses were analyzed in a 2 (Oxy: HbO and HbR) × 2 (Cond: Standard and No-Conflict) ANOVA separately for *Switchers* and *Perseverators*. Note that data from *Switchers* only included correct trials, but data from *Perseverators* included correct No-Conflict trials and incorrect Standard trials.

7 | RESULTS

This event-related task elicited the expected pattern of performance (see Figure 7): *Switchers* performed well across both conditions (*t*(26)

TABLE 1 Number of included participants and average number of trials per condition across regions. Regions required at least six participants to be analyzed

	Perseverators		Switchers	
Region	*n*	Avg tr	*n*	Avg tr
F5	14	9.7	25	14.3
F6	14	8.4	24	14.0
F7	6	7.5	15	8.5
F8	8	6.9	18	9.8
P3	10	5.1	18	8.3
P5	8	6.4	12	9.8
P6	6	8.3	17	8.4
T3	6	6.9	16	10.7

= 1.60, *ns*), but *Perseverators* sorted significantly better in the No-Conflict condition compared to the Standard condition ($t(14) = 6.00$, $p < .001$). Interestingly, *Perseverators* also performed poorly in the Total Change condition. This condition has only been reported one other time, and 3-year-olds performed better in the Total Change condition compared to the Standard condition (Zelazo et al., 2003). Children may have performed more poorly in our task due to the additional task demands of repeatedly switching between sets of rules. From the perspective of the model, the Total Change task lacks bottom-up support from memory that is present in the No-Conflict condition; this may explain *Perseverator*'s poorer performance.

Channels were defined as showing task-related activation if a significant Oxy effect or Oxy*Cond interaction was present (see Buss, Fox et al., 2014). Table 2 shows the ANOVA results. *Perseverators* showed diffuse Oxy effects across bilateral frontal cortex. Examination of these channels revealed larger HbR signals relative to HbO on all channels except the F5 cluster which showed a pattern indicating activation of this cortical region (i.e., HbO > HbR). *Switchers* showed an Oxy effect focused on a single channel in the F5 cluster. Examination of the data showed that HbO was larger than HbR, suggesting that *Switchers* activated this region of cortex when switching rules. Follow-up analyses on data from the single frontal channel common to both groups revealed that *Switchers* showed a significantly stronger HbO response compared to *Perseverators* during the time-window from 1 to 5 s post trial onset ($t(37) = 2.06$, $p < .05$). That is, *Switchers* activated left frontal cortex more strongly than *Perseverators*, replicating results from Moriguchi and Hiraki (2009).

The same frontal channel that replicated effects from Moriguchi and Hiraki also showed a significant Oxy*Cond interaction for *Perseverators*. Follow-up analyses showed a significantly stronger frontal HbO response in the No-Conflict condition compared to the Standard condition ($t(13) = 2.41$, $p < .05$), consistent with the first model prediction that *Perseverators* would more strongly activate frontal cortex when switching in the No-Conflict condition compared to when perseverating in the Standard condition (see Figure 8b, top left panel). Next, *Switchers* showed robust task-related activation in both temporal and parietal channels (see Figure 8b, middle right and bottom right panels); no significant task-related activation was observed in temporal or parietal cortex for *Pereverators* (see Figure 8b, middle left and bottom left panels). This is consistent with the second model prediction that developmental improvements in the Standard condition would be associated with activation of posterior cortical regions. Finally, follow-up analyses on the Oxy*Cond interactions in temporal ($t(15) = 2.18$, $p < .05$ for T31; $t(15) = 2.40$, $p < .05$ for T32; $t(15) = 1.79$, *ns* for T33) and parietal ($t(16) = 2.37$, $p < .05$ for P62) channels for *Switchers* showed a stronger HbO response in the No-Conflict condition (see dashed red lines in Figure 8b) compared to the Standard condition (see solid red line in Figure 8b). This is consistent with model predictions that *Switchers* would show stronger activation in posterior cortical regions in the No-Conflict condition compared to the Standard condition.

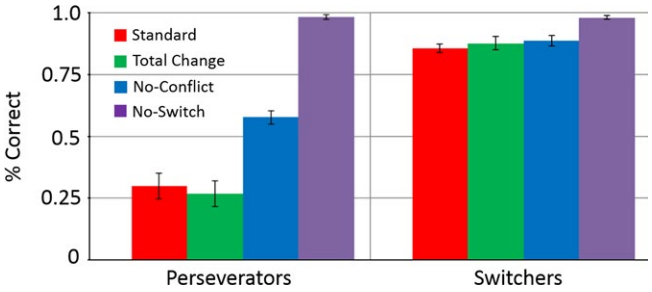

FIGURE 7 Behavioral results. Average percent correct across conditions for valid switch trials. Error bars represent standard error of the mean

8 | DISCUSSION

In our study, we classified children as *Switchers* or *Perseverators* based on their performance in the Standard condition. *Switchers* performed equally well in the Standard and No-Conflict conditions whereas *Perseverators* performed significantly better in the No-Conflict condition compared to the Standard condition. In the Standard condition, *Switchers* showed significantly stronger activation in left frontal cortex compared to the *Perseverators*. As predicted by the DNF model, *Perseverators* showed stronger activation in left frontal cortex when correctly switching in the No-Conflict condition compared to when perseverating in the Standard condition. Results were also consistent with two additional predictions of the model: *Switchers* showed activation in parietal and temporal cortex and activation in these regions was stronger in the No-Conflict condition compared to the Standard condition.

These results provide the first task-based, functional neuroimaging perspective on cortical-cortical interactions as EF develops. Previous data from Moriguchi and Hiraki (2009) suggest that children who fail the standard DCCS task have an immature frontal cortex that is the cause of their inflexibility. Our novel design enabled comparison across multiple conditions within the same group of participants, revealing that frontal cortex is reliably engaged when children correctly switch rules, *even in early childhood*.

TABLE 2 Results of the omnibus ANOVAs. Results shown for $p < .05$

Omnibus ANOVA channel	Perseverators		Switchers	
	Effect	F(*df*-effect,*df*-error)	Effect	F(*df*-effect,*df*-error)
Frontal				
F5-1	HbX*Cond	$F(1, 13)=4.69$	HbX	$F(1, 24)=10.83$
F5-2	HbX*Cond	$F(1, 13)=14.79$		
F5-3	HbX*Cond	$F(1, 13)=8.26$		
F6-1	HbX	$F(1, 13)=7.94$		
F6-3	HbX*Cond	$F(1, 13)=4.90$		
F7-2	HbX*Cond	$F(1, 5)=8.54$		
F7-3	HbX*Cond	$F(1, 5)=9.75$		
F8-1	HbX	$F(1, 7)=6.46$		
Parietal				
P6-2			HbX Cond	$F(1, 16)=5.01$ $F(1, 16)=4.84$
Temporal				
T3-1			HbX*Cond	$F(1, 15)=4.43$
T3-2			HbX*Cond	$F(1, 15)=8.03$
T3-3			HbX*Cond	$F(1, 15)=4.61$

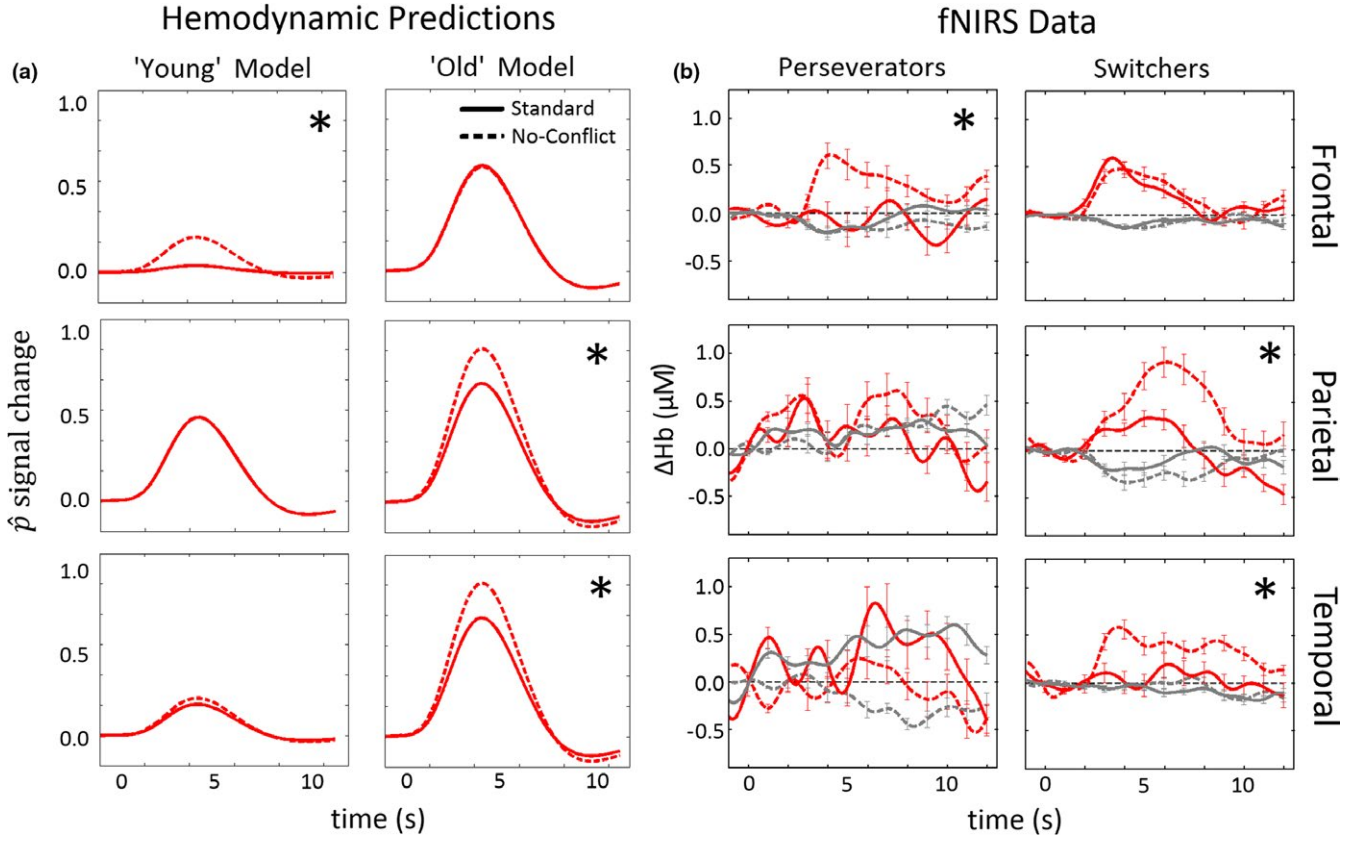

FIGURE 8 fNIRS results. (a) Reproduction of the hemodynamic predictions of the DNF model from Figure 3. (b) Group average hemodynamic response for the time-window from 1 second before the onset of a trial up to 12 s post onset of a trial. Oxy-Hb data are plotted in red and Deoxy-Hb data are plotted in gray. Oxy- and Deoxy-Hb data were averaged from a time-window spanning 2 s post stimulus to 10 s post stimulus for ANOVA analyses. Asterisks mark regions that showed significant Oxy × Condition interactions in the ANOVA

Three-year-olds, who showed weak frontal activation when perseverating in the Standard DCCS task, nonetheless showed robust frontal activation when correctly switching rules in an "easy" version (i.e., the No-Conflict version) of the same task. These data demonstrate that cognitive theories of EF focusing solely on frontal cortex growth are incomplete. According to these theories, activation

within frontal cortex is determined by the developmental state of this brain region. By contrast, the DNF model implements cortical-cortical neural interactions, providing a formal framework for thinking about how changes in frontal-posterior coupling can give rise to 3-year-olds' fragile EF skills. Specifically, bottom-up influences from posterior cortical areas can drive frontal cortex activation in the No-Conflict condition, reflecting the lack of cortical competition in this "easy" task. Critically, this lack of neural conflict was also evident in *Switchers*, but as a top-down effect from frontal cortex to posterior cortices.

A key question raised by our findings is how these effects emerge in development? We created development in the model by giving the "young" and "old" models different parameters. But how do these parameters change in a real brain? The literature is currently dominated by theories that make little contact with experience-dependent processes (Bunge & Zelazo, 2006; Morton, 2010). We argue that our findings point toward an exciting alternative explanation grounded in learning labels for visual features and dimensions. Specifically, a label learning process could provide structure for the long-range connections between frontal and posterior regions as label representations in frontal cortex are connected to feature representations in temporal cortex. For example, as frontal representations are consistently co-activated with posterior representations (e.g., the consistent activation of a label for "blue" and the activation of neural units tuned to the blue hue), these connections between labels and features become stronger. Over time, this could build a semantic network that can guide attention toward task-relevant features based on the activation of labels.

The results in the "easy" version of the DCCS task suggest that posterior cortical regions can provide on-the-job training for frontal cortex, sending a strong bottom-up signal to frontal. This process creates an optimal situation for Hebbian learning that could serve to strengthen patterns of frontal-posterior connectivity. For example, associating a label representation with a visual feature requires the co-activation of a label and feature. Due to the "young" model having a weakly engaged frontal system, learning can be more challenging when the frontal system is only weakly activated and does not provide a clear signal isolating specific synaptic connections that should be strengthened. By getting an extra boost of activity from the posterior system, the frontal system can be put into an activated state which may provide a basis for more robust learning to occur.

Additional work using the DNF model reported here illustrates how pre-exposure to features can lead to stronger activation of the dimensional units. In this example, children played a memory game with the post-switch features before beginning the Standard DCCS task. In the model, this memory game built a distributed set of memory traces within the feature field that would be relevant for the post-switch phase. Three-year-olds with extra pre-exposure to features show improved switching during the post-switch phase of the Standard DCCS task (S. Perone et al., 2015). It is an open question whether this prior experience with the memory game changes frontal cortex activation in the context of the DCCS task. This could be tested directly with fNIRS using the methods described here.

The data presented in the present report provide a hopeful path forward for intervention work. The fNIRS data revealed different conditions in the DCCS task that resulted in differences in frontal cortex activation for children who were classified as *Perseverators*, suggesting that cortical activation is open to task-specific experience. Thus, neural assessments might help identify experiences that can be used to tune posterior and frontal systems in the brain. For example, do children who engage frontal cortex repeatedly in the context of the "easy" version of the DCCS show more rapid developmental improvements in the "hard" version of the task? The model predicts that such a situation repeated over many iterations would lead to developmental improvements that should extend beyond the DCCS task. In this way, DNF models can be used to generate effective training regimes for EF skills that could have a positive impact for at-risk children.

ACKNOWLEDGEMENT

We thank Gregor Schöner for helpful comments on this work.

CONFLICTS OF INTEREST

The authors declare no competing financial interests.

REFERENCES

Anderson, J.R., Qin, Y., Jung, K.-J., & Carter, C.S. (2007). Information-processing modules and their relative modality specificity. *Cognitive Psychology*, *54*, 185–217.

Boas, D.A., & Franceschini, M. (2009). Near infrared imaging. *Scholarpedia*, *4*, 6997.

Boas, D.A., Gaudette, T., Strangman, G., Cheng, X., Marota, J.J., & Mandeville, J.B. (2001). The accuracy of near infrared spectroscopy and imaging during focal changes in cerebral hemodynamics. *NeuroImage*, *13*, 76–90.

Bunge, S.A., & Zelazo, P.D. (2006). A brain-based account of the development of rule use in childhood. *Psychological Science*, *15*, 118–121.

Buss, A.T., Fox, N., Boas, D.A., & Spencer, J.P. (2014). Probing the early development of visual working memory capacity with functional near-infrared spectroscopy. *NeuroImage*, *85*, 314–325.

Buss, A.T., & Spencer, J.P. (2014). The emergent executive: A dynamic neural field theory of the development of executive function. *Monographs of the Society for Research in Child Development*, *79*, 1–104.

Buss, A.T., Wifall, T., Hazeltine, E., & Spencer, J.P. (2014). Integrating the behavioral and neural dynamics of reponse selection in a dual-task paradigm: A dynamic neural field model of Dux et al. (2009). *Journal of Cognitive Neuroscience*, *26*, 334–351.

Carlson, S.M. (2005). Developmentally sensitive measures of executive function in preschool children. *Developmental Neuropsychology*, *28*, 595–616.

Diamond, A., & Lee, K. (2011). Interventions shown to aid executive function development in children 4 to 12 years old. *Science*, *333*, 959–964.

Eakin, L., Minde, K., Hechtman, L., Ochs, E., Krane, E., Bouffard, R., & Looper, K. (2004). The marital and family functioning of adults with ADHD and their spouses. *Journal of Attention Disorders*, *8*, 1–10.

Ezekiel, F., Bosma, R., & Morton, J.B. (2013). Dimensional Change Card Sort performance associated with age-related differences in functional connectivity of lateral prefrontal cortex. *Developmental Cognitive Neuroscience*, *5*, 40–50.

Fair, D.A., Cohen, A.L., Dosenbach, N.U.F., Church, J.A., Miezin, F.M., Barch, D.M., & Schlaggar, B.L. (2008). The maturing architecture of the brain's default network. *Proceedings of the National Academy of Sciences of the United States of America*, *105*, 4028–4032.

Fair, D.A., Dosenbach, N.U.F., Church, J.A., Cohen, A.L., Brahmbhatt, S., Miezin, F.M., & Schlaggar, B.L. (2007). Development of distinct control networks through segregation and integration. *Proceedings of the National Academy of Sciences of the United States of America*, *104* (33), 13507–12.

Heckman, B.J.J. (2011). The economics of inequality: The value of early childhood education. *American Educator*, *35* (31–36), 47.

Herd, S.A., Banich, M.T., & O'Reilly, R.C. (2006). Neural mechanisms of cognitive control: An integrative model of Stroop task performance and FMRI data. *Journal of Cognitive Neuroscience*, *18*, 22–32.

Huppert, T.J., Diamond, S.G., Franceschini, M.A., & Boas, D.A. (2009). HomER: A review of time-series analysis methods for near-infrared spectroscopy of the brain. *Applied Optics*, *48*, 1–33.

Logothetis, N.K., Pauls, J., Augath, M., Trinath, T., & Oeltermann, A. (2001). Neurophysiological investigation of the basis of the fMRI signal. *Nature*, *412*, 150–157.

Moffitt, T.E., Arseneault, L., Belsky, D., Dickson, N., Hancox, R.J., Harrington, H., & Caspi, A. (2011). A gradient of childhood self-control predicts health, wealth, and public safety. *Proceedings of the National Academy of Sciences of the United States of America*, *108*, 2693–2698.

Moriguchi, Y., & Hiraki, K. (2009). Neural origin of cognitive shifting in young children. *Proceedings of the National Academy of Sciences of the United States of America*, *106*, 6017–6021.

Morton, J.B. (2010). Understanding genetic, neurophysiological, and experiential influences on the development of executive functioning: The need for developmental models. *Wiley Interdisciplinary Reviews: Cognitive Science*, *1*, 709–723.

Morton, J.B., Bosma, R., & Ansari, D. (2009). Age-related changes in brain activation associated with dimensional shifts of attention: An fMRI study. *NeuroImage*, *46*, 249–256.

Morton, J.B., & Munakata, Y. (2002). Active versus latent representations: A neural network model of perseveration, dissociation, and decalage. *Developmental Psychobiology*, *40*, 255–265.

Perone, S., Molitor, S., Buss, A.T., Spencer, J.P., & Samuelson, L.K. (2015). Inducing dimensional attention in the dimensional change card sort task. *Child Development*, *86*, 812–827.

Perone, S., Plebanek, D.J., Lorenz, M.G., Spencer, J.P., & Samuelson, L.K. (2017). Empirical tests of a brain-based model of executive function development. *Child Development*, https://doi.org/10.1111/cdev.12885

Schroeter, M.L., Zysset, S., Wahl, M., & von Cramon, D.Y.Y. (2004). Prefrontal activation due to Stroop interference increases during development: An event-related fNIRS study. *NeuroImage*, *23*, 1317–1325.

Wijeakumar, S., Ambrose, J.P., Spencer, J.P., & Curtu, R. (2017). Model-based functional neuroimaging using dynamic neural fields: An integrative cognitive neuroscience approach. *Journal of Mathematical Psychology*, *76*, 212–235.

Zelazo, P.D. (2006). The Dimensional Change Card Sort (DCCS): A method of assessing executive function in children. *Nature Protocols*, *1*, 297–301.

Zelazo, P.D., Muller, U., Frye, D., & Marcovitch, S. (2003). The development of executive function in early childhood. *Monographs of the Society for Research in Child Development*, *68*, 1–137.

SUPPORTING INFORMATION

Additional Supporting Information may be found online in the supporting information tab for this article.

How to cite this article: Buss AT, Spencer JP. Changes in frontal and posterior cortical activity underlie the early emergence of executive function. *Dev Sci*. 2017;e12602. https://doi.org/10.1111/desc.12602